Targeting AXL and the DNA Damage Response Pathway as a Novel Therapeutic Strategy in Melanoma

Karine Flem-Karlsen[1,2], Erin McFadden[1], Nasrin Omar[3], Mads H. Haugen[3], Geir Frode Øy[3], Truls Ryder[4], Hans Petter Gullestad[4], Robert Hermann[4], Gunhild Mari Mælandsmo[3,5], and Vivi Ann Flørenes[1]

ABSTRACT

Receptor tyrosine kinase AXL is found upregulated in various types of cancer, including melanoma, and correlates with an aggressive cancer phenotype, inducing cell proliferation and epithelial-to-mesenchymal transition. In addition, AXL has recently been linked to chemotherapy resistance, and inhibition of AXL is found to increase DNA damage and reduce expression of DNA repair proteins. In light of this, we aimed to investigate whether targeting AXL together with DNA damage response proteins would be therapeutically beneficial. Using melanoma cell lines, we observed that combined reduction of AXL and CHK1/CHK2 signaling decreased proliferation, deregulated cell-cycle progression, increased apoptosis, and reduced expression of DNA damage response proteins. Enhanced therapeutic effect of combined treatment, as compared with mono-treatment, was further observed in a patient-derived xenograft model and, of particular interest, when applying a three-dimensional *ex vivo* spheroid drug sensitivity assay on tumor cells harvested directly from 27 patients with melanoma lymph node metastases. Together, these results indicate that targeting AXL together with the DNA damage response pathway could be a promising treatment strategy in melanoma, and that further investigations in patient groups lacking treatment alternatives should be pursued.

Introduction

The incidence of melanoma is increasing worldwide (1). While the prognosis of early-stage disease is very good, once the cancer progress survival drops dramatically, with over 20,000 melanoma-related deaths in Europe annually (2). Approximately 50% of all melanomas harbor activating BRAF mutations, with $BRAF^{V600E}$ being the most prevalent. The development of $BRAF^{V600}$ inhibitors vemurafenib and dabrafenib has led to targeted treatment options for patients with these mutations. However, almost all patients develop resistance within a year, often due to reactivation of the MAPK pathway or other receptor tyrosine kinases independently of BRAF (3, 4). Lately, immune checkpoint inhibitors, like mAbs targeting PD-1 and CTLA-4, have shown promising therapeutic effects (5). Yet, only a portion of the patients respond, signifying the importance to identify alternative therapeutic strategies.

The receptor tyrosine kinase AXL; a 138-kDa single-pass transmembrane protein of the TYRO3, AXL, MERTK (TAM) family, has been found overexpressed, both as mRNA and protein, in a wide range of cancers (6–8), including melanoma (9). AXL is reported to play a role in cancer progression, and has been shown to promote cell proliferation, migration, invasion, and epithelial-to-mesenchymal transition (EMT) (10–13). In addition, AXL has shown to mediate resistance to BRAF and MEK inhibitors (14, 15) as well as immunotherapy (16). All the TAM family members are activated by the vitamin K–dependent ligand growth arrest–specific protein 6 (GAS6), with AXL having the highest affinity for the ligand (17). In addition, AXL can be activated independently of GAS6 through aggregation of the protein or by heterodimerization with non-TAM receptor tyrosine kinases (18). Activated AXL undergoes homodimerization and autophosphorylation to induce downstream effects that activate proteins involved in the PI3K, MAPK14 (p38/MAPK), and MAPK1 (ERK/MAPK) pathways (12, 13, 19).

Recently, AXL expression was found to reduce the sensitivity to chemotherapies, as well as to PARP inhibitors (20–22). In ovarian cancer cell lines, an association between AXL and cisplatin resistance has been observed (23). In addition, inhibited AXL expression has been found to induce DNA damage and reduce the expression of DNA damage repair proteins (21). Together, these data suggest a link between AXL and the DNA damage response (DDR) pathway. Central to the DDR are the serine/threonine–specific kinases CHK1 and CHK2 that are activated by ATR or ATM, respectively, in response to single-stranded (ATR) or double-stranded (ATM) DNA breaks. CHK1 and CHK2 transduce signals to effectors such as TP53 (p53), CDC25C, BRCA1, and RAD51, ultimately leading to DNA repair, cell-cycle arrest, and/or apoptosis (24).

In this study, we assessed how dual inhibition of AXL and CHK1/CHK2 altered proliferation, signal transduction, apoptosis, and cell-cycle distribution in melanomas. We discovered that targeting or inhibiting expression of AXL and CHK1/CHK2 in combination reduced cell proliferation and induced cell-cycle arrest and apoptosis. We further showed that the combined treatment was superior to mono-treatment in a patient-derived xenograft (PDX) model and when analyzing drug sensitivity utilizing cells harvested directly from melanoma lymph node metastases in a 3D *ex vivo* drug efficacy assay. Together, these data suggest that dual targeting of AXL and DDR pathway is a promising treatment strategy for melanomas that should be further investigated in patients having developed resistance and where few treatment alternatives are available.

[1]Department of Pathology, The Norwegian Radium Hospital, Oslo University Hospital, Oslo, Norway. [2]Institute for Clinical Medicine, Faculty of Medicine, University of Oslo, Oslo, Norway. [3]Department of Tumor Biology, Institute for Cancer Research, The Norwegian Radium Hospital, Oslo University Hospital, Oslo, Norway. [4]Department of Plastic and Reconstructive Surgery, The Norwegian Radium Hospital, Oslo University Hospital, Oslo, Norway. [5]Institute of Medical Biology, Faculty of Health Sciences, UiT–Arctic University of Norway, Tromsø, Norway.

Note: Supplementary data for this article are available at Molecular Cancer Therapeutics Online (http://mct.aacrjournals.org/).

Corresponding Author: Karine Flem-Karlsen, The Norwegian Radium Hospital, Oslo University Hospital, Ullernchausseen 66-68, Oslo 0379, Norway. Phone: 474-541-4387; E-mail: kaflem@rr-research.no

Mol Cancer Ther 2020;19:895–905

doi: 10.1158/1535-7163.MCT-19-0290

Materials and Methods

Cell lines and patient material

Melanoma cell lines were established from subcutaneous (Melmet 1) or lymph node (Melmet 5, FEMX-1 and HHMS) metastatic lesions of patients treated at the Norwegian Radium Hospital, Oslo University Hospital (Oslo, Norway; refs. 25, 26). WM115, WM902B, WM983, and WM1366 cells were a kind gift from Meenhard Herlyn, the Wistar cell line collection. The melanoma cell lines MDA-MB-435 and MeWo were obtained from ATCC. All cells were routinely checked for *Mycoplasma* by PCR in-house. Melmet 1 and WM1366 cell lines were STR fingerprinted (April 2018) by Genetica Cell Line Testing. The melanoma cells were grown in RPMI1640 (Sigma Aldrich) supplemented with 5% FBS (Sigma Aldrich) and 2 mmol/L L-glutamine (Lonza). Cells were maintained in a humidified incubator at 37°C and with 5% CO_2. All cells were used within 20 passages of thawing.

Melanoma lymph node metastases were obtained from patients operated at the Norwegian Radium Hospital, Oslo University Hospital (Oslo, Norway). Patient material was collected with written informed consent in accordance with the Declaration of Helsinki. The study was approved by the Norway Regional Committee for Medical and Health Research Ethics (approval number 2014/2208 and 2015/2434).

Immunoblot, protein analysis, and antibodies

Protein extracts and immunoblots were performed as described previously (27), with the following exceptions: proteins were lysed in a buffer containing 1% Triton X-100, 50 mmol/L Hepes (pH 7.4), 150 mmol/L NaCl, 1.5 mmol/L $MgCl_2$, 1 mmol/L EGTA, 100 mmol/L NaF, 10 mmol/L sodium pyruvate, 1 mmol/L Na_3VO_4, and 10% glycerol, with addition of 10 μL/mL protease and phosphatase inhibitor cocktails (cOmplete Mini and PhosSTOP, Roche). Antibodies used were: pAXL (#5724), AXL (#8661), pAKT (#9271), AKT (#9272), pERK (#9101), pp38 (#9211), p38 (#8690), pSRC (#12432), SRC (#2108), pp53 (#9284), p53 (#2524), CDKN1A (p21) (#2947), pCDC25C (#9528), CDC25C (#4688), pCHK1 (#2341), CHK1 (#2360), pCHK2 (#2661), CHK2 (#6334; all diluted 1:1,000, Cell Signaling Technology), ERK2 (D2; #sc-1647, 1:1,000, Santa Cruz Biotechnology), and α-tubulin (DM1A; #05-829, 1:50,000, Millipore). Protein bands were visualized by SuperSignal West Dura Extended Duration Substrate (Thermo Fisher Scientific) and exposed in a Syngene G Box. If not otherwise specified, protein lysates were made from cells that had been subjected to 400 ng/mL GAS6 (R&D Systems) and 10 μg/mL Vitamin K (Sigma Aldrich) for 60 minutes. USA Simple Western immunoassay was performed according to the manufacturer protocol and run on the Peggy Sue machine (ProteinSimple). Antibodies used were AXL (1:100, #8661 Cell Signaling Technology) and β-actin (1:300, #4967 Cell Signaling Technology). Data were analyzed using the Compass Software (ProteinSimple).

Reagents

BGB324 (previously known as R428, first described in ref. 28) was a kind gift from BerGenBio. AZD7762 (first described in ref. 29, catalog no. S1532) and VE-822 (first described in refs. 30, 31; compound 45, see company website, catalog no. S7102, for updated structure) was purchased from SelleckChemicals. Inhibitors, diluted in DMSO, were used at concentrations and time periods indicated, with controls receiving the same amount of DMSO as the treatment groups.

RNA interference

Cells were transfected with 100 nmol/L siRNA using Lipofectamine 2000 in Opti-MEM Media (Thermo Scientific) according to the manufacturer's protocol using the following siRNAs targeting AXL: 3 unique 27mer siRNA duplexes (catalog no.: SR319445, Origene) and ON-TARGETplus Human *AXL* siRNA (catalog no.: J-003104-13-0002, Dharmacon), CHK1: ON-TARGETplus Human *CHEK1* siRNA (catalog nos. J-003255-10-0002 and J-003255-11-0002, Dharmacon), and CHK2: ON-TARGETplus Human *CHEK2* siRNA (catalog nos. J-003256-17-0002 and J-003256-18-0002, Dharmacon). ON-TARGETplus Non-targeting Pool Control siRNA (catalog no. D-001810-10-05, Dharmacon) was used as control. Cells were left for 48 hours before they were used in further experiments.

In vitro proliferation and caspase-3/7 cleavage

For analyzing the effect on proliferation, cells were plated at 15%–25% confluency in 96-well or 6-well culture plates and left overnight before treatment with drugs for 72 hours. Cell confluence was visualized by IncuCyte FLR or IncuCyte Zoom Kinetic Imaging System (Essen Bioscience) light scanning microscopes. For colony formation assays, 500 or 1,000 cells were plated in 6-well culture plates overnight before drug-containing media was added. After 21 days, colonies were fixated with ice-cold methanol before being stained with 0.05% crystal violet and counted using the GelCount machine (Oxford Optronix).

Caspase-3/7 cleavage was determined using the CellPlayer 96-well Caspase-3/7 reagent (Essen Bioscience) according to the manufacturer's protocol. In brief, cells were plated to yield 10%–20% confluency. The following day, drugs and 2.5 μmol/L caspase-3/7 reagent was added. Caspase-3/7 cleavage, yielding fluorescent signals, was visualized by IncuCyte FLR or IncuCyte Zoom Kinetic Imaging System (Essen Bioscience) light scanning microscopes. Fluorescence was related to the confluence of the respective well at the respective time points.

Flow cytometry

Cells were plated at 30% confluency in 6-well plates overnight before incubation with BGB324 and/or AZD7762 for 24 hours. Control cells were treated with DMSO. Harvested cells were fixated in 70% ice-cold methanol and stored at −20°C for at least 24 hours. Cells were then labeled with 2.4 μL/mL Hoechst 33258 (Sigma Aldrich) or 500 μL propidium iodide Cycloscope Reagent (Cytognos) and incubated for 10 minutes shielded from light. H2AX staining was performed on fixed cells resuspended and blocked in detergent buffer [0.1% Nonidet P40 (Igepal CA-630), 6.5 mmol/L Na_2HPO_4, 1.5 mmol/L KH_2PO_4, 2.7 mmol/L KCL, 137 mmol/L NaCl, 0.5 mmol/L EDTA PH 7.5 with 4% nonfat milk] before primary incubation with γH2AX antibody (1:500, Abcam) and secondary incubation with Alexa Fluor 647 antibody (1:500, Abcam). Cells were labeled with 2.4 μL/mL Hoechst 33258 (Sigma Aldrich). Analysis was performed using the LSRII flow cytometer (BD Biosciences) and analyzed by FlowJo v10 software.

Invasion and migration assays

To measure cell invasion, 50 μg Matrigel (BD Biosciences) was added to Falcon Transparent PET Membrane 24-well 8.0-μm cell culture inserts (Corning). Newly split cells were incubated with 0.1 mCi/mL ^{3}H-Thymidine (Nerliens Mezansky) for 24 hours. Thereafter, 50,000 serum-starved ^{3}H-Thymidine-labeled cells/well were plated in the inserts, in RPMI1640 media (Sigma Aldrich) containing drugs, but without serum. Five percent FBS was added to the bottom well in addition to drugs in the same concentration as the top well. Cells were harvested by scraping from the bottom and top of the Matrigel with a cotton swab that was further inserted into tubes containing 4 mL Aquasafe 300 scintillation fluid (Zinsser Analytic). The invasive ability was determined by comparing ^{3}H-Thymidine-radioactivity as a

measure of number of cells on the bottom of the Matrigel membrane divided by the total radioactivity of cells from top and bottom of the membrane.

Migration was measured by plating 50,000 cells/well in 96-well culture plates and scratching the wells the following day by The WoundMaker 96-well pin block (Essen Biosciences) before adding drug. Cell migration was determined using the Incucyte FLR or Incuzoom Zoom Kinetic Imaging System (Essen Biosciences), that scan the cells every 3 hours, and with the respective software calculating cell confluence.

Ex vivo drug sensitivity assay

Melanoma lymph node metastases obtained following surgery were disaggregated for 1 hour by 125 U collagenase type 2 (Sigma Aldrich) and 2.5 mg/mL DNase (Sigma Aldrich). To remove aggregates and debris, the cell suspensions were filtered through 100 μmol/L filters (WVR). If necessary, red blood cells were removed using ACK lysing buffer (Lonza). Live cells (15,000–20,000 per well) were seeded in Nunc 96-Well Polystyrene Round Bottom Microwell plates (Thermo Fisher Scientific) in RPMI1640 (Sigma Aldrich) medium supplemented with 5% FBS, 2 mmol/L L-glutamine, 100 U/mL penicillin, and 0.1 mg/mL streptomycin (all Lonza) and allowed to form three-dimensional spheroids. Drugs were added at indicated concentrations immediately after seeding and the cells incubated for 5 days before viability was measured using the CellTiter-Glo Luminescent Cell Viability Assay (Promega), and analyzed by Fluoroscan Ascent Fl (Thermo Fisher Scientific). The *ex vivo* assay was performed once for each patient sample, with at least three technical replicates per condition.

In vivo studies

Eight-week-old female athymic (foxn1 nu) nude mice were injected subcutaneously with 2×10^6 Melmet 1 cells in the right flank. When the tumors reached a volume of approximately 50 mm^3, the mice were randomized into four groups containing 6–8 mice in each group. 50 mg/kg BGB324 diluted in 0.5% hydroxypropyl methylcellulose/0.1% Tween-80 was given twice daily by oral gavage and 25 mg/kg AZD7762 diluted in 11.3% (2-Hydroxypropyl)-β-cyclodextrin was given intravenously three times a week. Treatment duration was 14 days. Groups not receiving BGB324 and/or AZD7762 were administered drug vehicles in the same manner as treatment groups. Treatment toxicity was monitored by weight loss measured twice daily on treatment and twice weekly off treatment. Mice with ≥15% reduced weight were euthanized. Tumor diameters were measured twice a week by digital calipers and tumor volume calculated by the formula $0.5 \times \text{length} \times \text{width}^2$. In line with governmental regulations, the mice were euthanized when the tumors reached a diameter of 16 mm and/or a volume of 2,000 mm^3. *In vivo* data is presented as average tumor volume + SEM. All mice were bred at the Department of Comparative Medicine, The Norwegian Radium Hospital (Oslo, Finland), housed in rooms with alternating light/dark cycles of 12 hours, had *ad libitum* access to food and water and were kept according to regulations of the Norwegian Animal Welfare Act. Animal experiments were approved by the Norwegian Animal Research Authority (FOTS approval number 8554).

Statistical analysis

All values represent data average + SD or SEM. Statistical significance was determined by student two-tailed *t* test when comparing two groups or one-way ANOVA when comparing three groups. Significance over various time points in the animal experiments was determined by AUC analysis. The statistical analyses were performed using GraphPad Prism version 7.0 (GraphPad Software). *P* values of less than 0.05 were considered significant and marked with asterisks, where *, $P < 0.05$; **, $P < 0.01$; and ***, $P < 0.001$. Synergism was calculated by the CalcuSyn Software (Biosoft) using the Chou-Talalay CI method (32). Experiments were performed at least three times with at least three technical replicates in each experiment, if not otherwise specified. Immunoblots were performed at least twice with independent lysates.

Results

Decreased expression or inhibition of AXL reduced proliferation and MAPK and PI3K signaling

Ten melanoma cell lines were first examined for AXL expression by Simple Western immunoassay (Supplementary Fig. S1A). Of the three AXL-expressing cell lines (Melmet 1, WM1366, and MeWo), the two with the highest expression (Melmet 1 and WM1366) were chosen for further studies. The impact of AXL on proliferation was investigated following transfection with two different small interfering RNAs (siRNA). As shown in **Fig. 1A**, silencing AXL decreased proliferation and reduced colony formation as compared with scrambled siRNA control. The effect on proliferation was further confirmed following treatment with the specific small-molecule AXL inhibitor BGB324 (ref. 28; **Fig. 1B**). A BGB324 concentration of 2 μmol/L was chosen as a higher dose (3 μmol/L) drastically reduced proliferation, suggesting off-target effects at this dose (Supplementary Fig. S1B). Because of the role of AXL in epithelial-to-mesenchymal transition (EMT; ref. 33), we next investigated the effect of AXL inhibition on migration and invasion. As shown in Supplementary Fig. S1C, treatment with BGB324 for 24 hours reduced migration and invasion in both cell lines.

To investigate the effect of targeting AXL on cell signaling, we first confirmed that GAS6 activates AXL, as demonstrated by increased Tyrosine 702 phosphorylation (Supplementary Fig. S1D). This phosphorylation site is found responsible for the general activation of the protein (34). BGB324 reduced AXL activation in a dose-dependent manner in both cell lines (**Fig. 1C**). Of particular note, BGB324 increased the total AXL protein level, suggesting an attempt to rescue the reduced AXL signaling. Next, the impact of AXL inhibition on downstream signaling pathways was examined. As demonstrated in **Fig. 1C**, BGB324 treatment in GAS6 stimulated cells decreased phosphorylation of AKT, ERK, and particularly SRC, but not p38. These effects were confirmed in siAXL-transfected cells (**Fig. 1D**).

Combined targeting of AXL and the DNA damage response pathway reduced viability and tumor growth in melanoma cell lines and patient-derived models

The newly discovered link between AXL signaling and DNA damage response (DDR; refs. 21, 35) spurred us to investigate the effect of combined inhibition of AXL and the DDR. As shown in **Fig. 2A** and **B**, cotreatment with BGB324 and the CHK1/2 inhibitor AZD7762 synergistically decreased proliferation in both Melmet 1 and WM1366 cells. The effect was validated using a 3D (spheroid) drug efficacy assay in Melmet 1 cells (**Fig. 2C**). To rule out the possibility of off-target effects, we treated the AXL-negative cell line WM115 with BGB324 and/or AZD7762 *in vitro* and using the spheroid drug sensitivity assay and only observed reduced proliferation mediated by the AZD7762 treatment (**Fig. 2D**), suggesting no off-target effects of the BGB324 treatment. Furthermore, reduced proliferation was also observed in siAXL cells treated with AZD7762 compared with treated and untreated scrambled control–transfected cells (**Fig. 2E**). The

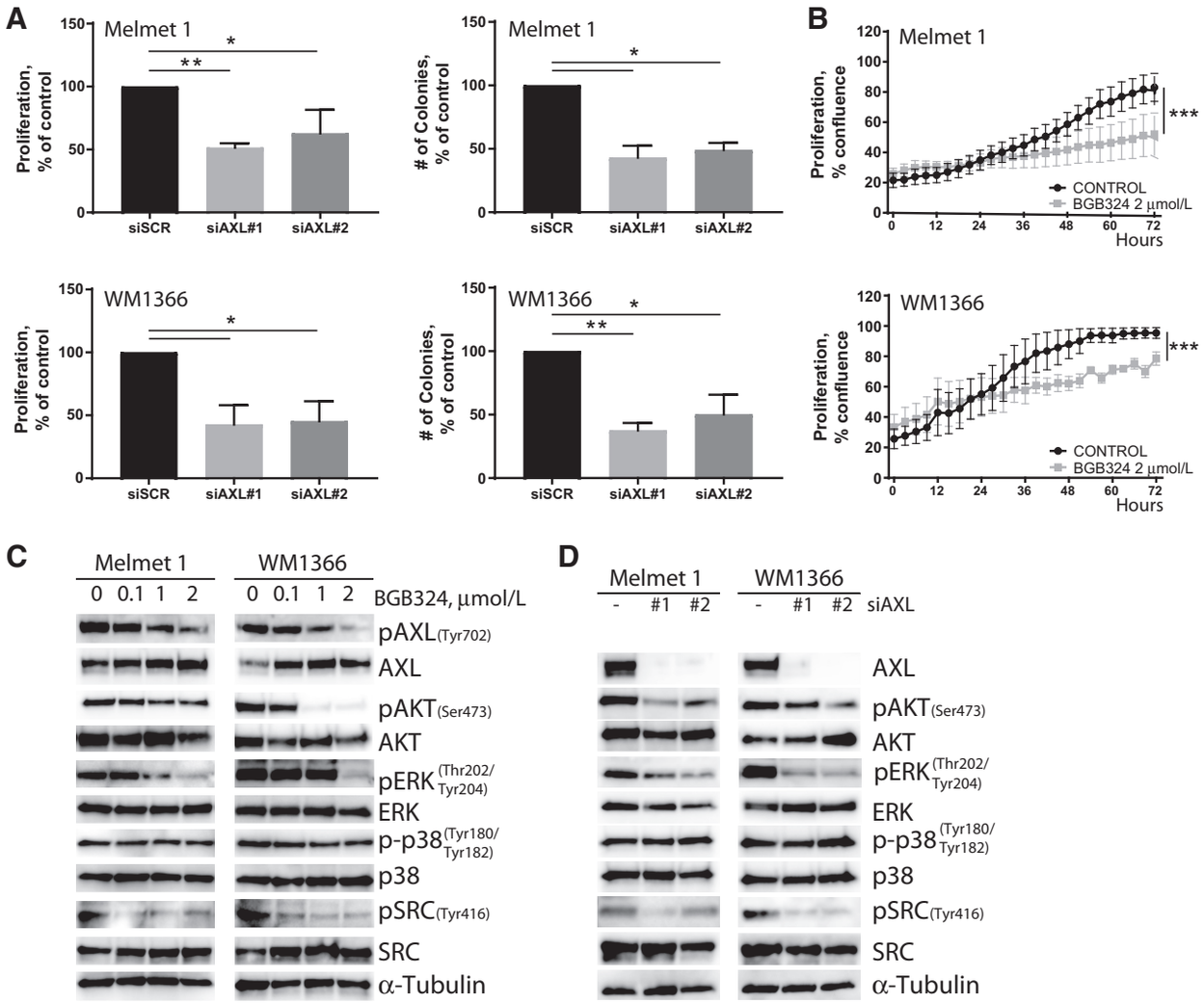

Figure 1.

Effects of diminished AXL expression or activity on cell proliferation and signaling. **A,** Proliferation of Melmet 1 and WM1366 cells with siRNA-mediated silencing of AXL expression measured by IncuCyte Live imaging 72 hours after plating ($n = 3$; left) or by colony formation 21 days after plating (right). Colony formation shows an average of two independent experiments for Melmet 1 cells and three independent experiments for WM1366 cells. **B,** Melmet 1 and WM1366 cells treated with 2 µmol/L BGB324 (AXL inhibitor) reduced proliferation as measured by the IncuCyte Live imaging system ($n = 3$). Representative immunoblot analysis of indicated proteins following treatment with indicated concentrations of BGB324 for 24 hours (**C**) and siRNA-mediated AXL silencing (**D**). Control cells were treated with DMSO (**C**) or scrambled siRNA (**D**). Immunoblots were performed at least twice with independent lysates (*, $P < 0.05$; **, $P < 0.01$; ***, $P < 0.001$).

transfected cells were more responsive to AZD7762 than untransfected cells (**Fig. 2A**), possibly due to the added stress of the transfection.

To elucidate whether the effect was dependent on either CHK1 or CHK2 signaling, we diminished CHK1 or CHK2 expression by siRNA before treating the cells with BGB324. Reduced expression of CHK1 or CHK2) resulted in slight to no change in proliferation compared with scrambled control–transfected cells (**Fig. 3A** and **B**). In both cell lines, siCHK1-transfected cells responded with decreased proliferation in combination with BGB324 compared with BGB324 treated and untreated control–transfected cells. This was only significant in cells where CHK1 was completely eradicated (siCHK1 #1), indicating that even a low expression of CHK1 is enough to partly protect the cells from growth inhibition. There was also lower proliferation in siCHK2-transfected cells treated with BGB324 compared with BGB324 treatment alone; however, only significant for one of the siRNA molecules (siCHK2 #1). Reducing expression of either CHK1 or CHK2 did not lead to as pronounced decrease in proliferation as AZD7762 treatment, neither alone nor in combination with BGB324, suggesting that signaling through both proteins must be abolished to maximize the response. To examine this hypothesis, we reduced the expression of both CHK1 and CHK2 and observed reduced proliferation in the siCHK1 and siCHK2 cells comparable with AZD7762 monotreatment (**Fig. 3C** and **D**). The proliferation of the combined siCHK1 and siCHK2-transfected cells was further reduced when the cells were treated with BGB324, yielding results in concordance with cells treated with BGB324 and AZD7762.

Furthermore, we aimed to determine whether reduced proliferation was only dependent on diminished activation of the

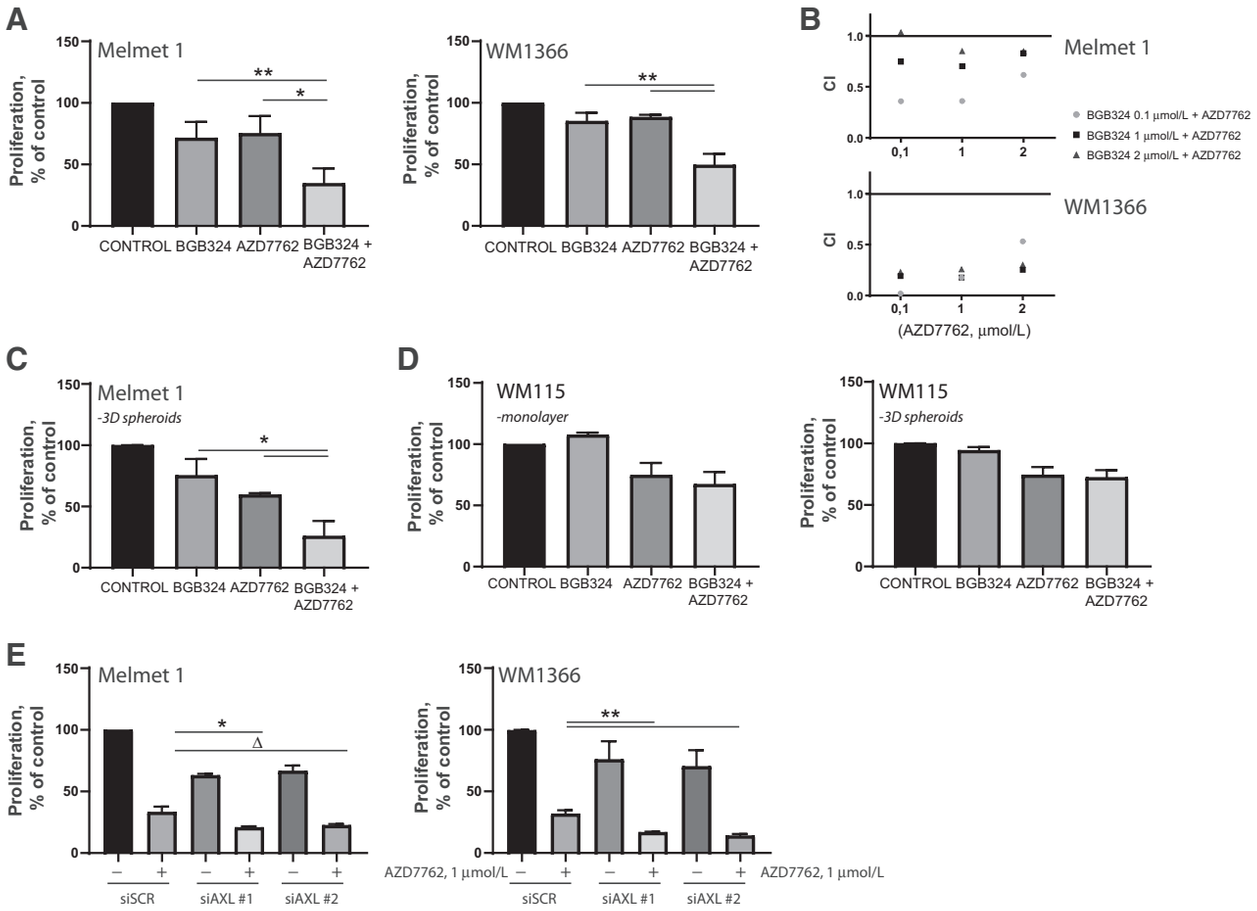

Figure 2.

Inhibition of AXL and CHK1 and CHK2 signaling reduced proliferation in melanoma cell lines. **A,** Dual treatment with 2 µmol/L BGB324 and 1 µmol/L AZD7762 reduced average proliferation in Melmet 1 and WM1366 melanoma cell lines. **B,** Combination index (CI) values as estimated by the Chou–Talalay method using average proliferation of indicated doses of BGB324 and AZD7762. CI < 1 indicates synergy. **C,** Proliferation of Melmet 1 cells treated with 2 µmol/L BGB324 and/or 1 µmol/L AZD7762 measured by the 3D spheroid assay correlates to what is observed *in vitro*. **D,** Proliferation measured by Incucyte Live imaging system (left) and using the 3D spheroid assay (right) in the AXL-negative cell line WM115 treated with BGB324 and/or AZD7762. **E,** Silenced AXL expression in combination with 1 µmol/L AZD7762 reduced proliferation. Δ equals *P* value = 0.07. Proliferation was measured 72 hours after drug addition by the Incucyte Live imaging system (*in vitro*) or after 5 days using CellTiter-Glo Luminescent assay (3D spheroid assay). Control cells were treated with DMSO. Experiments show an average of three biological replicates + SEM (*, $P < 0.05$; **, $P < 0.01$).

CHK1/2 proteins or if similar effect could be observed when the activation of other DDR proteins was lowered. Thus, we inhibited signaling of ATR, mainly working upstream of CHK1, but also shown to activate CHK2 (36), using the ATR inhibitor VE-822 (refs. 30, 31; compound 45) in combination with BGB324 (**Fig. 3E**). In both cell lines, combinatorial treatment with VE-822 and BGB324 significantly inhibited cell proliferation compared with each mono-treatment. This illustrates that other proteins in the DDR pathway also could be targeted together with AXL and reduced cell proliferation. Overall, these data demonstrate that inhibiting or reducing the expression of AXL in combination with CHK1 and CHK2 or other proteins in the DDR pathway result in decreased cell viability.

The observed effect on proliferation upon simultaneous targeting of AXL and the DDR encouraged us to examine if this could also reduce proliferation in patient samples. To this end, cells harvested directly from 27 melanoma lymph node metastases were treated with BGB324 and AZD7762 alone or in combination and analyzed for effect on viability using the *ex vivo* drug sensitivity assay. As shown in **Fig. 4A**, the mean effects of the mono-treatments were slightly reduced compared with control; however, these results were not significant. BGB324 and AZD7762 in combination, however, significantly decreased the viability compared with either mono-treatment. Of note, cells from three of the patient tumor samples showed increased viability when treated with AZD7762 alone, and in two of them, the viability was not reduced following combined treatment. Finally, the superior effect of the combined treatment was confirmed in the mouse Melmet 1 xenograft model (**Fig. 4B** and **C**). Whereas the mono-treated mice displayed insignificant reductions in tumor volume, mice treated with the combination showed significantly decreased relative tumor volume and prolonged survival time compared with untreated controls or following mono-treatments. No significant weight loss was observed indicating that the treatments were well tolerated (Supplementary Fig. S2).

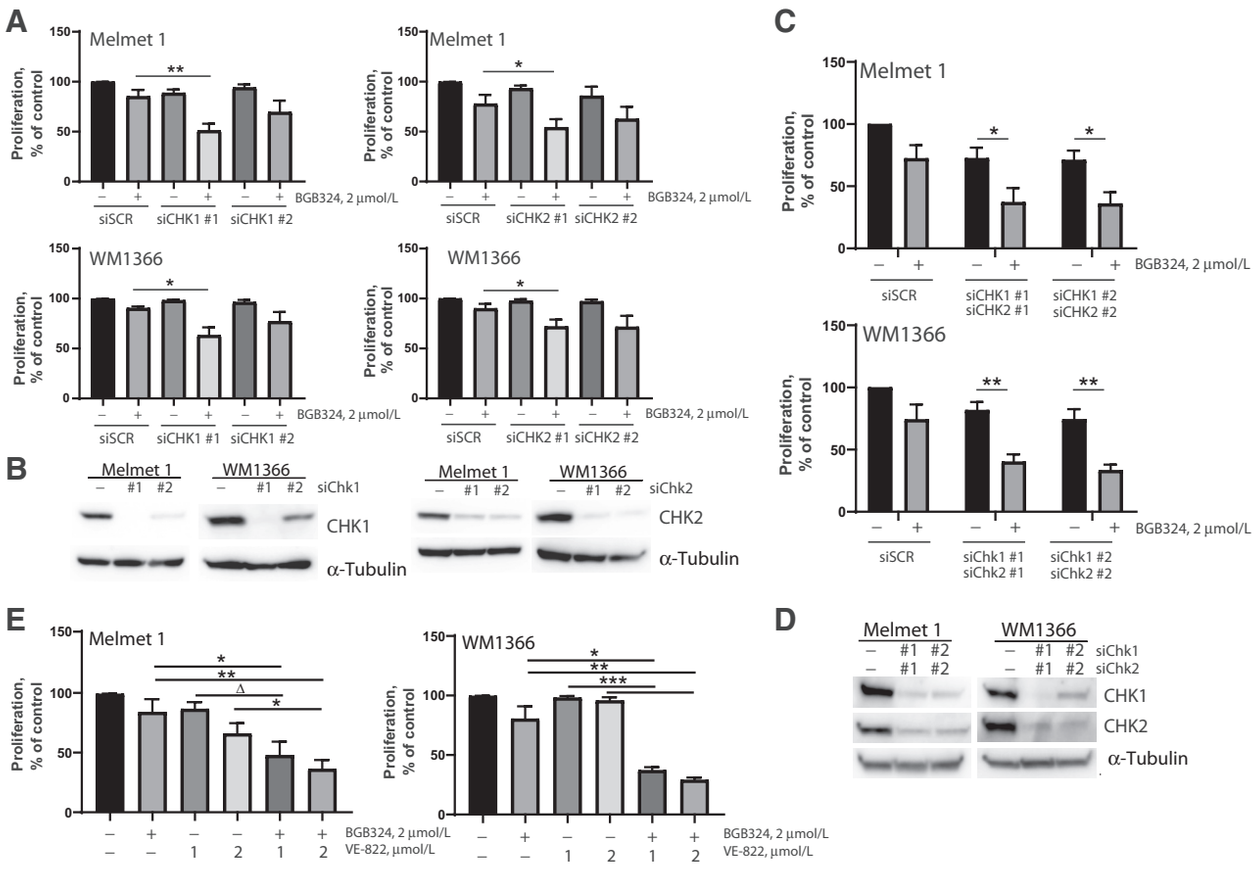

Figure 3.

Treatment with BGB324 and siCHK1 and/or siCHK2 or the ATR inhibitor VE-822 reduced cell proliferation. **A,** siRNA-mediated silencing of CHK1 (left) or CHK2 (right) before treatment with BGB324 reduced proliferation in melanoma cell lines. **B,** Immunoblot of CHK1 or CHK2 protein expression in cells transfected with siRNAs targeting either CHK1 (left) or CHK2 (right). **C,** Diminished expression of both CHK1 and CHK2 further reduced proliferation in combination with BGB324 treatment. **D,** Immunoblot of CHK1 and CHK2 expression in cells transfected with siCHK1 and siCHK2. **E,** Proliferation after drug addition of BGB324 and indicated doses of the ATR inhibitor VE-822. All proliferation data were measured by Incucyte Live imaging, and the data show average values relative to control cells calculated 72 hours after drug addition of at least three independent experiments + SEM. BGB324: 2 μmol/L. Control cells were treated with DMSO. *, $P < 0.05$; **, $P < 0.01$; ***, $P < 0.001$; Δ equals $P = 0.0512$).

Combined inhibition of AXL and CHK1/CHK2 leads to cell-cycle arrest and increased apoptosis

Because of the observed effects on proliferation and viability, we aimed to investigate how reduced AXL and CHK1/2 activity alone and in combination affected cell-cycle progression and apoptosis. As shown in **Fig. 5A** and Supplementary Fig. S3A, BGB324 treatment had no effect on cell-cycle progression in any of the cell lines. AZD7762 treatment, on the other hand, slightly increased the S-phase fraction in Melmet 1 cells at both 24 and 48 hours posttreatment, but had minimal effect in WM1366 cells. Combining the two inhibitors, however, resulted in a considerable S-phase arrest in Melmet 1 cells at 24 hours, and S-phase and G_2–M phase arrest at 48 hours. Cotreatment of WM1366 cells led to G_2–M arrest at both 24 hours and 48 hours, whereas S-phase arrest was only observed after 48 hours.

In addition, in both cell lines, a marked sub-G_1 peak, suggesting apoptosis or necrosis, was observed (Supplementary Fig. S3B) following combined treatment with BGB324 and AZD7762. To analyze whether this reflected apoptosis, cleavage of caspase-3 and caspase-7 was examined using a kit yielding a fluorescent signal upon cleavage. As shown in **Fig. 5B** (left), mono-treatments slightly increased cleavage of caspase-3 and -7, while this was significantly augmented following the combined treatment. Caspase-3 cleavage was further confirmed by Western blot analysis (**Fig. 5B**, right), demonstrating caspase-3 cleavage induced by AZD7762 and further increased in cells receiving the combined treatment. However, no caspase-3 cleavage was observed in BGB324-treated cells as examined by Western blot analysis. This is in contrast to the BGB324-induced cleavage of caspase-3 and -7 observed by the apoptosis assay, suggesting that caspase-7 cleavage plays a more prominent role following BGB324 treatment.

Furthermore, we investigated the molecular effects of BGB324 and/or AZD7762 treatments by Western blot analyses. As seen in **Fig. 5C**, both compounds alone and in combination reduced the phosphorylation of AXL and increased the expression of total AXL. This is in agreement with previous reports demonstrating that AZD7762 may reduce AXL phosphorylation (37). Also in line with previous reports (38), AZD7762 increased phosphorylation of CHK1 and CHK2 in both cell lines, indicating activation of the DDR pathway. In addition, AZD7762 increased Serine 216 phosphorylation of CDC25C, a downstream effector of CHK1 and CHK2.

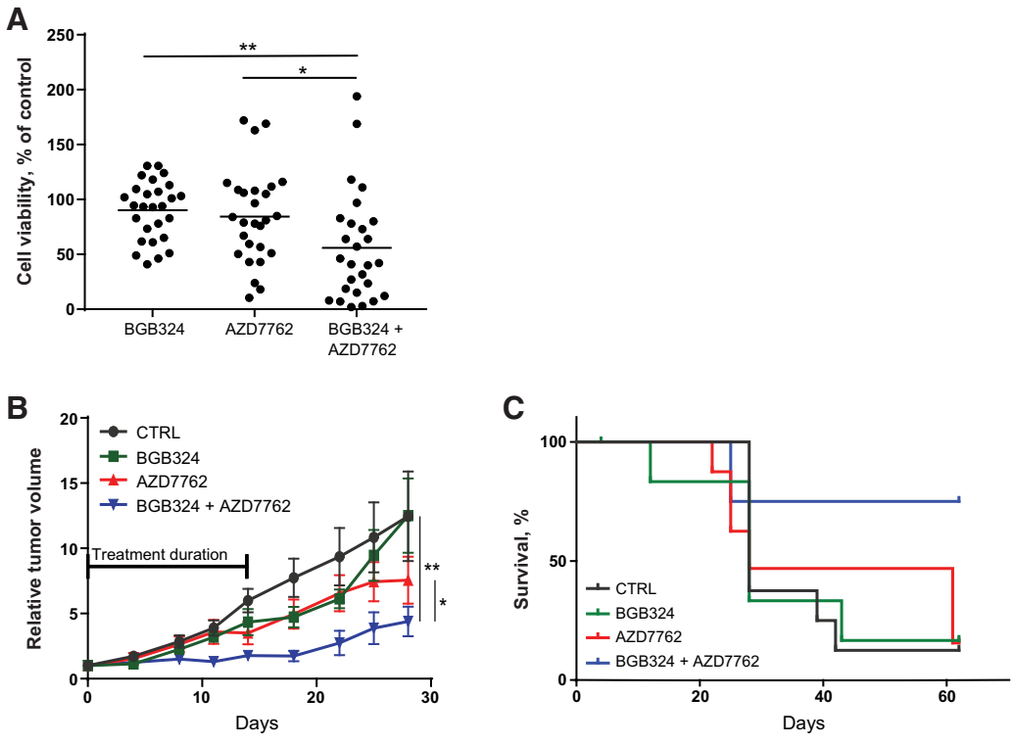

Figure 4.

Dual inhibition of AXL and CHK1/2 reduced cell viability in patient tumor samples and inhibited tumor growth *in vivo*. **A,** Lymph node metastases from melanoma patients were disaggregated, and cells were plated as spheres and treated with 2 μmol/L BGB324 and/or 2 μmol/L AZD7762 for 5 days. Cell viability was measured by CellTiter-Glo and related to control samples treated with DMSO ($n = 27$ patients). **B,** Tumor volume relative to the volume at day of treatment initiation of Melmet 1 xenografts treated with 50 mg/kg BGB324 twice daily and/or 25 mg/kg AZD7762 three times a week for 2 weeks. Controls were treated with drug vehicle(s). There were 6 to 8 mice per group. **C,** Kaplan–Meier survival curve showing percentage of mice in **B** still alive as function of time. The experiment was terminated at day 62, and all mice still alive ($n = 9$) were censored. *, $P < 0.05$; **, $P < 0.01$.

While BGB324 treatment alone did not show any effect on CHK1 and CHK2 phosphorylation compared with control, CDC25C was greatly phosphorylated. Phosphorylation and total expression of CHK1, CHK2, and CDC25C was reduced in the combined treatment.

Previous reports have suggested that BGB324 induces activation and expression of H2AFX (H2AX; ref. 21). This was not evident in our cell lines (**Fig. 5C**). H2AX phosphorylation and expression was, however, observed in AZD7762-treated cells and further increased following combined treatment. The H2AX immunoblot results were verified by flow cytometry for WM1366 cells (Supplementary Fig. S3C).

BGB324 alone had no effect on expression of the DDR proteins p53 or CDKN1A ($p21^{WAF1/Cip1}$) in any of the two cell lines, whereas AZD7762 and the combination increased p53 protein levels as well as Serine 15 phosphorylation in Melmet 1 cells (p53 wild-type). Surprisingly, increased serine 15 phosphorylation of p53 was also observed in the p53-mutated cell line WM1366 after treatment with AZD7762 alone and in combination with BGB324. In both cell lines, AZD7762 increased the expression of $p21^{WAF1/Cip1}$ and this was further augmented when the two inhibitors were combined. While both monotreatments decreased PI3K and MAPK signaling, enhanced reduction when combined was only seen in PI3K signaling in Melmet 1 cells (Supplementary Fig. S3D). These data were also observed in cells treated with BGB324 and/or VE-822 (Supplementary Fig. S3E). Importantly, VE-822 treatment reduced pAXL expression (Supplementary Fig. S3E), which was also observed in AZD7762-treated cells (**Fig. 5C**). Furthermore, short (10 minutes) exposure to AZD7762 or VE-822 monotherapy did not reduce pAXL expression to the extent of BGB324 treatment (Supplementary Fig. S3F).

Together, our data indicate that targeting AXL in combination with the DDR pathway reduces proliferation, leads to downregulation of DDR response proteins, and ultimately results in apoptosis. Thus, targeting AXL together with the DDR could be a beneficial treatment option in melanoma.

Discussion

AXL has been observed overexpressed in various types of cancer and linked to aggressive tumor traits, poor prognosis, and drug resistance (33, 39). In melanoma, acquired resistance to MAPK inhibitors (14, 40) and immunotherapy (16) has been associated with increased AXL expression, making AXL an interesting target to overcome treatment resistance. AXL has also emerged as a promising therapeutic strategy in other types of cancers, and currently the AXL inhibitor BGB324 is in phase I/II clinical trials alone or in combination with chemotherapy (NCT02488408), erlotinib (NCT02424617), pembrolizumab (NCT03184558 and NCT03184571), or dabrafenib and trametinib (NCT02872259).

In accordance with a previous report (41), AXL was found expressed in 30% of the examined melanoma cell lines, and reducing (42, 43) or inhibiting (20) AXL expression modestly reduced proliferation, migration, and invasion. Inhibition of AXL led to decreased AXL-Tyrosine

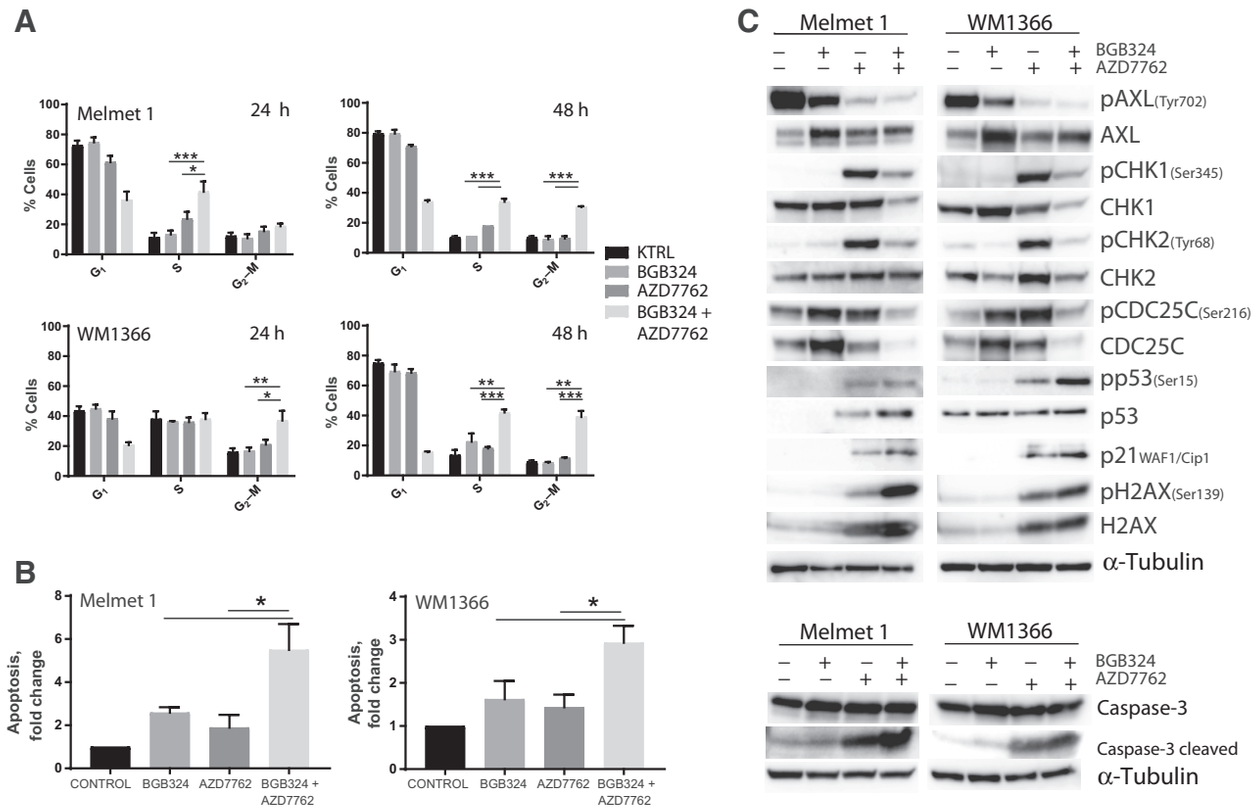

Figure 5.

Combined treatment of BGB324 and AZD7762 leads to cell-cycle arrest and apoptosis with reduced expression of cell-cycle regulators. **A,** Cell-cycle distribution of Melmet 1 and WM1366 treated with BGB324 and/or AZD7762 for 24 or 48 hours measured by Hoechst 33258 incorporation and analyzed by flow cytometry. The data are shown as average of three independent experiments for 24 hours and two independent experiments for 48 hours + SEM. **B,** Average apoptosis measured by fluorescence staining of a caspase-3/7 reagent by IncuCyte Live imaging. Fluorescent intensity was related to number of cells in each well and to control 72 hours after treatment with BGB324 and/or AZD7762 (left). Apoptosis experiments show an average of three biological experiments + SEM. Protein expression in total lysates of Melmet 1 and WM1366 cells treated with BGB324 and/or AZD7762 as shown by a representative immunoblot for proteins indicated (right). **C,** Protein expression in total lysates of Melmet 1 and WM1366 cells treated with BGB324 and/or AZD7762 for 24 hours as shown by a representative immunoblot for proteins indicated. Immunoblots were performed at least twice with independent lysates. In all experiments, control cells were treated with DMSO. Concentration of BGB324: 2 μmol/L and AZD7762: 1 μmol/L (*, $P < 0.05$; **, $P < 0.01$; ***, $P < 0.001$).

702 phosphorylation, indicating less activation of the protein (44). Furthermore, AXL has been found to activate the PI3K and MAPK pathways to induce prosurvival and proliferative signals (13). In accordance with this, we observed less proliferation and reduced phosphorylation of SRC, AKT, and ERK upon diminished expression or inhibition of AXL. It has been shown that SRC activity is dependent on partnerships with receptor tyrosine kinases such as EGFR and PDGFR (45). These receptor tyrosine kinases are closely related to AXL and the substantial decrease in pSCR expression at even low levels of BGB324 treatment indicate that SRC activity may be dependent on AXL signaling as well. In contrast to what has been observed by others (46), no effect on p38/MAPK signaling was observed, potentially due to cell line or cancer type specific differences in p38/MAPK–mediated stress signaling.

Recently, inhibition of AXL signaling was found to induce DNA damage (21, 35) and it has also been proposed that AXL protect cancer cells from fork collapse (35), which is mediated by ATR/ATM-CHK1/2 signaling. In this study, we neither observed activation of H2AX nor CHK1/2 following BGB324 treatment, suggesting that inhibiting AXL does not induce DNA damage in our melanoma cell lines. On the other hand, BGB324 led to increased inhibitory phosphorylation (Serine 216) of CDC25C, implying cell-cycle arrest. CHK1/2 signaling was not activated by BGB324 treatment, suggesting that CDC25C is inhibited independently of CHK1/2, for instance, through phosphorylation by MARK3 (c-TAK1), p38/MAPK, CAMK2A, and PRKA (AMPK), as has been reported by others (47, 48). In addition, CHK1/2-independent phosphorylation of CDC25C-Serine 216 must also hold true for AZD7762-treated cells as this inhibitor blocks the downstream signaling of CHK1/2 by acting as an ATP competitor (29).

Because of a prior article describing effects of AXL on DDR (21), we speculated whether treatment with BGB324 in combination with a DDR inhibitor could be a beneficial therapeutic strategy in melanoma. In support of this, we found that targeting AXL together with CHK1 and CHK2 inhibited proliferation and viability in cell cultures, PDX models, and patient material. Decreased proliferation was coupled with cell-cycle deregulation and increased apoptosis. These data are in accordance with a previous finding showing that inhibition of AXL in combination with WEE1, a regulator of cell-cycle progression downstream of CHK1/2, reduced tumor growth and increased apoptosis in

small-cell lung cancer cells (49). While knockdown of CHK1 or CHK2 resulted in reduced proliferation in combination with BGB324, the effect was not as pronounced as when inhibiting or reducing the expression of both CHK1 and CHK2. This suggests that redundancy, crosstalk, and overlapping roles of CHK1 and CHK2 (50) protect the cells from growth inhibition when targeting only one of the proteins.

It has previously been shown that AZD7762 treatment reduces AXL phosphorylation (37), a finding in accordance with our results. A direct influence of AZD7762 on AXL phosphorylation might suggest that the inhibitory effect on proliferation when combining the two inhibitors solely is caused by decreased AXL activity. In a kinase screen of AZD7762, the drug also showed selectivity toward AXL, although it was ten times lower for AXL than CHK1/2 (29). To rule out the possibility of AZD7762 affecting AXL signaling, we diminished CHK1 or CHK2 expression, or treated cells with an ATR inhibitor (VE-822), in combination with BGB324. These experiments led to similar results as when using the AZD7762 and BGB324 inhibitors. Importantly, decreased pAXL expression was also observed in cells treated with VE-822, suggesting that there is some unknown mechanism of the DDR pathway that indirectly or directly targets AXL signaling. This interpretation in strengthened by the observation that AZD7762 or VE-822 did not reduce pAXL expression to that of BGB324-treated cells in a short (10 minutes) exposure to the drugs. These data demonstrate that the observed consequences of the combined treatment are not due to off-target effects of the AZD7762 inhibitor. Surprisingly, in the scrambled-transfected control cells, we observed lower proliferation when the cells were treated with AZD7762 (**Fig. 2E**) compared with the same treatment in untransfected cells (**Fig. 2A**). This effect was not observed in control transfected cells treated with BGB324 (**Fig. 3A**). We do not know the reason for this, but it is shown that lipofectamine treatment increases DNA damage and induces cellular stress (51, 52). Thus, we speculate that DNA damage and cellular stress produced by the transfection will sensitize the cells for the AZD7762 treatment hindering DDR and inducing cellular toxicity. Despite this, cellular proliferation was even further decreased after treatment with AZD7762 in combination with AXL knockdown.

We show here that while AZD7762 treatment resulted in activation and expression of DDR proteins such as CHK1, CHK2, and CDC25C, combined treatment with BGB324 diminished the expression of these proteins, implying that AXL facilitates the DDR. In line with this, AXL inhibition in combination with inhibitors of the DNA repair protein PARP or the cell-cycle regulator WEE1 has shown to reduce the expression of DDR and DNA repair proteins (21, 49). Furthermore, previous reports have shown that accumulation of p53 and $p21^{WAF1/Cip1}$ following DNA damage is associated with reduced expression of CHK1 (53), CHK2 (54), and CDC25C (55), which was also observed in this study. We do not know, however, if the accumulation of p53 and $p21^{WAF1/Cip1}$ precedes the downregulation of DDR protein expression, or if the downregulation of these proteins promotes increased p53 and $p21^{WAF1/Cip1}$ activation and/or expression. p53 and $p21^{WAF1/Cip1}$ activation and/or expression play a role in triggering apoptosis, and in line with this, we observed that the combined inhibition of AXL and CHK1/2 led to apoptosis through cleavage of caspase-3 and -7. AZD7762 treatment caused a more pronounced increase in caspase-3 cleavage, as assessed by immunoblot, than BGB324 treatment, while the caspase-3 and -7 cleavage was approximately similar in the two mono-treatments as measured by the fluorescent reagent. This indicates that BGB324 activates caspase-7 to a larger degree than AZD7762 treatment.

The observed effects on cell viability upon combined AXL and CHK1/2 targeting in cell lines, was further verified using disaggregated cells from melanoma lymph node metastases in an *ex vivo* drug efficacy assay. The added effect of the combined treatment relative to the mono-treatments was less pronounced in the *ex vivo* assay, probably due to the presence of nonmalignant cells in the lymph node metastases or by cells that do not express AXL. Despite this, the assay clearly distinguishes patient-derived tumor cells with different sensitivity to the applied drugs. Previously, we have confirmed platinum chemotherapy resistance in patients with ovarian cancer (56), and recently we demonstrated concordance between response to the mutated BRAF inhibitor vemurafenib and *BRAF/NRAS* mutation status when analyzing tumor cells from melanoma lymph node metastases in the *ex vivo* assay (57). Together, these data show that the *ex vivo* assay is able to reflect patient response to various drugs, and should be further evaluated as a supplement to guide treatment in patients having developed resistance against standard treatment regimes.

To conclude, AXL is shown to be upregulated in melanoma and its expression is associated with treatment resistance, making AXL an interesting target to overcome resistance to therapy. In this study, we investigated the effect of targeting AXL together with the DDR and found that this combination resulted in reduced cell proliferation and tumor growth. We show that dual inhibition of AXL and the DDR result in cell-cycle retention and increased apoptosis through downregulation of CHK1, CHK2, and CDC25C, suggesting that AXL facilitate the DDR. These data strongly suggest that targeting AXL together with the DDR may be a promising treatment strategy for melanoma and studies to further investigate this possibility is highly warranted.

Disclosure of Potential Conflicts of Interest

No potential conflicts of interest were disclosed.

Authors' Contributions

Conception and design: K. Flem-Karlsen, G.M. Mælandsmo, V.A. Flørenes
Development of methodology: K. Flem-Karlsen
Acquisition of data (provided animals, acquired and managed patients, provided facilities, etc.): K. Flem-Karlsen, E. McFadden, T. Ryder, H.P. Gullestad, R. Hermann
Analysis and interpretation of data (e.g., statistical analysis, biostatistics, computational analysis): K. Flem-Karlsen, N. Omar
Writing, review, and/or revision of the manuscript: K. Flem-Karlsen, E. McFadden, M.H. Haugen, H.P. Gullestad, G.M. Mælandsmo, V.A. Flørenes
Administrative, technical, or material support (i.e., reporting or organizing data, constructing databases): E. McFadden, V.A. Flørenes
Study supervision: G.M. Mælandsmo, V.A. Flørenes
Other (performed experiments): G.F. Øy

Acknowledgments

We thank Prof. Meenhard Herlyn for the WM115, WM902b, WM983, and WM1366 cell lines and BerGenBio for kindly granting us BGB324. We thank Karianne Giller Fleten, Monica Bostad, and Elisabeth Emilsen for technical assistance. This work was supported by the Southern and Eastern Norway Regional Health Authority (to K. Flem-Karlsen and E. McFadden).

The costs of publication of this article were defrayed in part by the payment of page charges. This article must therefore be hereby marked *advertisement* in accordance with 18 U.S.C. Section 1734 solely to indicate this fact.

Received March 19, 2019; revised August 28, 2019; accepted December 10, 2019; published first December 23, 2019.

References

1. Rigel DS. Epidemiology of melanoma. Semin Cutan Med Surg 2010;29:204–9.
2. Ferlay J, Steliarova-Foucher E, Lortet-Tieulent J, Rosso S, Coebergh JW Comber H, et al. Cancer incidence and mortality patterns in Europe: estimates for 40 countries in 2012. Eur J Cancer 2013;49:1374–403.
3. Gibney GT, Messina JL, Fedorenko IV, Sondak VK, Smalley KS. Paradoxical oncogenesis–the long-term effects of BRAF inhibition in melanoma. Nat Rev Clin Oncol 2013;10:390–9.
4. Hatzivassiliou G, Song K, Yen I, Brandhuber BJ, Anderson DJ, Alvarado R, et al. RAF inhibitors prime wild-type RAF to activate the MAPK pathway and enhance growth. Nature 2010;464:431–5.
5. Ott PA, Hodi FS, Robert C. CTLA-4 and PD-1/PD-L1 blockade: new immunotherapeutic modalities with durable clinical benefit in melanoma patients. Clin Cancer Res 2013;19:5300–9.
6. Jin G, Wang Z, Wang J, Zhang L, Chen Y, Yuan P, et al. Expression of Axl and its prognostic significance in human breast cancer. Oncol Lett 2017;13:621–8.
7. Sun W, Fujimoto J, Tamaya T. Coexpression of Gas6/Axl in human ovarian cancers. Oncology 2004;66:450–7.
8. Yu H, Liu R, Ma B, Li X, Yen HY, Zhou Y, et al. Axl receptor tyrosine kinase is a potential therapeutic target in renal cell carcinoma. Br J Cancer 2015;113:616–25.
9. Quong RY, Bickford ST, Ing YL, Terman B, Herlyn M, Lassam NJ. Protein kinases in normal and transformed melanocytes. Melanoma Res 1994;4:313–9.
10. Paccez JD, Vasques GJ, Correa RG, Vasconcellos JF, Duncan K, Gu X, et al. The receptor tyrosine kinase Axl is an essential regulator of prostate cancer proliferation and tumor growth and represents a new therapeutic target. Oncogene 2013;32:689–98.
11. Rankin EB, Fuh KC, Taylor TE, Krieg AJ, Musser M, Yuan J, et al. AXL is an essential factor and therapeutic target for metastatic ovarian cancer. Cancer Res 2010;70:7570–9.
12. Asiedu MK, Beauchamp-Perez FD, Ingle JN, Behrens MD, Radisky DC, Knutson KL. AXL induces epithelial-to-mesenchymal transition and regulates the function of breast cancer stem cells. Oncogene 2014;33:1316–24.
13. Gay CM, Balaji K, Byers LA. Giving AXL the axe: targeting AXL in human malignancy. Br J Cancer 2017;116:415–23.
14. Muller J, Krijgsman O, Tsoi J, Robert L, Hugo W, Song C, et al. Low MITF/AXL ratio predicts early resistance to multiple targeted drugs in melanoma. Nat Commun 2014;5:5712.
15. Rambow F, Rogiers A, Marin-Bejar O, Aibar S, Femel J, Dewaele M, et al. Toward minimal residual disease-directed therapy in melanoma. Cell 2018;174:843–55.
16. Hugo W, Zaretsky JM, Sun L, Song C, Moreno BH, Hu-Lieskovan S, et al. Genomic and transcriptomic features of response to anti-PD-1 therapy in metastatic melanoma. Cell 2016;165:35–44.
17. Zagorska A, Traves PG, Lew ED, Dransfield I, Lemke G. Diversification of TAM receptor tyrosine kinase function. Nat Immunol 2014;15:920–8.
18. Korshunov VA. Axl-dependent signalling: a clinical update. Clin Sci 2012;122:361–8.
19. Rankin EB, Fuh KC, Castellini L, Viswanathan K, Finger EC, Diep AN, et al. Direct regulation of GAS6/AXL signaling by HIF promotes renal metastasis through SRC and MET. Proc Natl Acad Sci U S A 2014;111:13373–8.
20. Brand TM, Iida M, Stein AP, Corrigan KL, Braverman CM, Coan JP, et al. AXL is a logical molecular target in head and neck squamous cell carcinoma. Clin Cancer Res 2015;21:2601–12.
21. Balaji K, Vijayaraghavan S, Diao L, Tong P, Fan Y, Carey JP, et al. AXL inhibition suppresses the DNA damage response and sensitizes cells to PARP inhibition in multiple cancers. Mol Cancer Res 2017;15:45–58.
22. Wilson C, Ye X, Pham T, Lin E, Chan S, McNamara E, et al. AXL inhibition sensitizes mesenchymal cancer cells to antimitotic drugs. Cancer Res 2014;74:5878–90.
23. Macleod K, Mullen P, Sewell J, Rabiasz G, Lawrie S, Miller E, et al. Altered ErbB receptor signaling and gene expression in cisplatin-resistant ovarian cancer. Cancer Res 2005;65:6789–800.
24. Smith J, Mun Tho L, Xu N, Gillespie DA. The ATM–Chk2 and ATR–Chk1 pathways in DNA damage signaling and cancer. In: Vande Woude GF, Klein G, editors. Advances in cancer research. Volume 108. Cambridge, MA: Academic Press; 2010. p. 73–112.
25. Fodstad O, Kjonniksen I, Aamdal S, Nesland JM, Boyd MR, Pihl A. Extrapulmonary, tissue-specific metastasis formation in nude mice injected with FEMX-I human melanoma cells. Cancer Res 1988;48:4382–8.
26. Prasmickaite L, Skrbo N, Hoifodt HK, Suo Z, Engebraten O, Gullestad HP, et al. Human malignant melanoma harbours a large fraction of highly clonogenic cells that do not express markers associated with cancer stem cells. Pigment Cell Melanoma Res 2010;23:449–51.
27. Magnussen GI, Holm R, Emilsen E, Rosnes AK, Slipicevic A, Florenes VA. High expression of Wee1 is associated with poor disease-free survival in malignant melanoma: potential for targeted therapy. PLoS One 2012;7:e38254.
28. Holland SJ, Pan A, Franci C, Hu Y, Chang B, Li W, et al. R428, a selective small molecule inhibitor of Axl kinase, blocks tumor spread and prolongs survival in models of metastatic breast cancer. Cancer Res 2010;70:1544–54.
29. Zabludoff SD, Deng C, Grondine MR, Sheehy AM, Ashwell S, Caleb BL, et al. AZD7762, a novel checkpoint kinase inhibitor, drives checkpoint abrogation and potentiates DNA-targeted therapies. Mol Cancer Ther 2008;7:2955–66.
30. Fokas E, Prevo R, Pollard JR, Reaper PM, Charlton PA, Cornelissen B, et al. Targeting ATR in vivo using the novel inhibitor VE-822 results in selective sensitization of pancreatic tumors to radiation. Cell Death Dis 2012;3:e441.
31. Charrier JD, Durrant SJ, Golec JM, Kay DP, Knegtel RM, MacCormick S, et al. Discovery of potent and selective inhibitors of ataxia telangiectasia mutated and Rad3 related (ATR) protein kinase as potential anticancer agents. J Med Chem 2011;54:2320–30.
32. Chou TC. Theoretical basis, experimental design, and computerized simulation of synergism and antagonism in drug combination studies. Pharmacol Rev 2006;58:621–81.
33. Gjerdrum C, Tiron C, Hoiby T, Stefansson I, Haugen H, Sandal T, et al. Axl is an essential epithelial-to-mesenchymal transition-induced regulator of breast cancer metastasis and patient survival. Proc Natl Acad Sci U S A 2010;107:1124–9.
34. Vouri M, Croucher DR, Kennedy SP, An Q, Pilkington GJ, Hafizi S. Axl-EGFR receptor tyrosine kinase hetero-interaction provides EGFR with access to pro-invasive signalling in cancer cells. Oncogenesis 2016;5:e266.
35. Kariolis MS, Miao YR, Diep A, Nash SE, Olcina MM, Jiang D, et al. Inhibition of the GAS6/AXL pathway augments the efficacy of chemotherapies. J Clin Invest 2017;127:183–98.
36. Matsuoka S, Rotman G, Ogawa A, Shiloh Y, Tamai K, Elledge SJ. Ataxia telangiectasia-mutated phosphorylates Chk2 in vivo and in vitro. Proc Natl Acad Sci U S A 2000;97:10389–94.
37. Park JS, Lee C, Kim HK, Kim D, Son JB, Ko E, et al. Suppression of the metastatic spread of breast cancer by DN10764 (AZD7762)-mediated inhibition of AXL signaling. Oncotarget 2016;7:83308–18.
38. Isono M, Hoffmann MJ, Pinkerneil M, Sato A, Michaelis M, Cinatl J Jr, et al. Checkpoint kinase inhibitor AZD7762 strongly sensitises urothelial carcinoma cells to gemcitabine. J Exp Clin Cancer Res 2017;36:1.
39. Liu L, Greger J, Shi H, Liu Y, Greshock J, Annan R, et al. Novel mechanism of lapatinib resistance in HER2-positive breast tumor cells: activation of AXL. Cancer Res 2009;69:6871.
40. Konieczkowski DJ, Johannessen CM, Abudayyeh O, Kim JW, Cooper ZA, Piris A, et al. A melanoma cell state distinction influences sensitivity to MAPK pathway inhibitors. Cancer Discov 2014;4:816–27.
41. Sensi M, Catani M, Castellano G, Nicolini G, Alciato F, Tragni G, et al. Human cutaneous melanomas lacking MITF and melanocyte differentiation antigens express a functional Axl receptor kinase. J Invest Dermatol 2011;131:2448–57.
42. Brand TM, Iida M, Stein AP, Corrigan KL, Braverman CM, Luthar N, et al. AXL mediates resistance to cetuximab therapy. Cancer Res 2014;74:5152–64.
43. Jiang C, Zhou L, Wang H, Zhang Q, Xu Y. Axl is a potential cancer prognostic marker for the migration and invasion of nasopharyngeal carcinoma. Adv Clin Exp Med 2016;25:531–7.
44. Schoumacher M, Burbridge M. Key roles of AXL and MER receptor tyrosine kinases in resistance to multiple anticancer therapies. Curr Oncol Rep 2017;19:19.
45. Irby RB, Yeatman TJ. Role of Src expression and activation in human cancer. Oncogene 2000;19:5636–42.
46. Corno C, Gatti L, Arrighetti N, Carenini N, Zaffaroni N, Lanzi C, et al. Axl molecular targeting counteracts aggressiveness but not platinum-resistance of ovarian carcinoma cells. Biochem Pharmacol 2017;136:40–50.
47. Hutchins JR, Clarke PR. Many fingers on the mitotic trigger: post-translational regulation of the Cdc25C phosphatase. Cell Cycle 2004;3:41–5.
48. Shen Y, Sherman JW, Chen X, Wang R. Phosphorylation of CDC25C by AMP-activated protein kinase mediates a metabolic checkpoint during cell-cycle G2/M-phase transition. J Biol Chem 2018;293:5185–99.

49. Sen T, Tong P, Diao L, Li L, Fan Y, Hoff J, et al. Targeting AXL and mTOR pathway overcomes primary and acquired resistance to WEE1 inhibition in small-cell lung cancer. Clin Cancer Res 2017;23:6239–53.
50. Bartek J, Lukas J. Chk1 and Chk2 kinases in checkpoint control and cancer. Cancer Cell 2003;3:421–9.
51. Fiszer-Kierzkowska A, Vydra N, Wysocka-Wycisk A, Kronekova Z, Jarzab M, Lisowska KM, et al. Liposome-based DNA carriers may induce cellular stress response and change gene expression pattern in transfected cells. BMC Mol Biol 2011;12:27.
52. Irianto J, Xia Y, Pfeifer CR, Athirasala A, Ji J, Alvey C, et al. DNA Damage follows repair factor depletion and portends genome variation in cancer cells after pore migration. Curr Biol 2017;27:210–23.
53. Gottifredi V, Karni-Schmidt O, Shieh S-Y, Prives C. p53 down-regulates CHK1 through p21 and the retinoblastoma protein. Mol Cell Biol 2001;21: 1066–76.
54. Matsui T, Katsuno Y, Inoue T, Fujita F, Joh T, Niida H, et al. Negative regulation of Chk2 expression by p53 is dependent on the CCAAT-binding transcription factor NF-Y. J Biol Chem 2004;279:25093–100.
55. Clair SS, Giono L, Varmeh-Ziaie S, Resnick-Silverman L, Liu WJ, Padi A, et al. DNA damage-induced downregulation of Cdc25C is mediated by p53 via two independent mechanisms: one involves direct binding to the cdc25C promoter. Mol Cell 2004;16:725–36.
56. Hetland TE, Kaern J, Skrede M, Sandstad B, Trope C, Davidson B, et al. Predicting platinum resistance in primary advanced ovarian cancer patients with an in vitro resistance index. Cancer Chemother Pharmacol 2012;69: 1307–14.
57. Florenes VA, Flem-Karlsen K, McFadden E, Bergheim IR, Nygaard V, Nygard V, et al. A three-dimensional ex vivo viability assay reveals a strong correlation between response to targeted inhibitors and mutation status in melanoma lymph node metastases. Transl Oncol 2019;12:951–8.